



Microwave-Assisted Metathetic Synthesis and Characterization of Fe₃O₄ Incorporated BaMoO₄:Er³⁺/Yb³⁺ Composites

CHANG SUNG LIM

Department of Advanced Materials Science & Engineering, Hanseo University, Seosan 356-706, South Korea

Corresponding author: Tel/Fax: +82 41 6601445; E-mail: cslim@hanseo.ac.kr

(Received: 19 July 2012;

Accepted: 6 May 2013)

AJC-13448

Fe₃O₄ incorporated Er³⁺/Yb³⁺ co-doped BaMoO₄ (BaMoO₄:Er³⁺/Yb³⁺) composites were successfully synthesized by a cyclic microwave-assisted metathetic route. The microstructure exhibited a well-defined and homogeneous morphology with sizes of 1-2 μm for the BaMoO₄:Er³⁺/Yb³⁺ particles and 0.1-0.5 μm for the Fe₃O₄ particles, respectively. The Fe₃O₄ particles were self-preferentially crystallized and immobilized on the surface of BaMoO₄:Er³⁺/Yb³⁺ particles. The synthesized Fe₃O₄ incorporated BaMoO₄:Er³⁺/Yb³⁺ composites were characterized by X-ray diffraction, scanning electron microscopy and energy-dispersive X-ray spectroscopy. Optical properties were examined by using photoluminescence emission data and Raman spectroscopy.

Key Words: Fe₃O₄; BaMoO₄:Er³⁺/Yb³⁺, Microwave assisted metathetic route, Photoluminescence, Raman spectroscopy.

INTRODUCTION

Fe₃O₄ incorporated photoluminescence composites containing two different functionalities could provide novel characteristics *via* the integration of fluorescent and magnetic properties, which offer a new potential in a wide range of applications in biomedical systems, such as targeted drug, diagnostic, therapeutics and bioimaging¹⁻³. Particles of rare earth-doped BaMoO₄, a type of metallic molybdate compound with a Scheelite-type structure of lattice parameters $a = b = 5.573 \text{ \AA}$ and $c = 12.786 \text{ \AA}$, are relatively stable in air and have stable physical and chemical properties, low excitation threshold energy and low-cost productivity⁴⁻⁶.

Recently, several processes have been developed to increase the applications of rare-earth-doped metal molybdates prepared using a range of processes, including solid-state reactions⁷⁻¹¹, co-precipitation¹², the sol-gel method¹³, the hydrothermal method¹⁴⁻¹⁶, the Pechini method¹⁷, the solvothermal route¹⁸ and the microwave-assisted hydrothermal method¹⁹. For practical application of photoluminescence in such products as lasers, three-dimensional displays, light emitting devices and biological detectors, features such as homogeneous particle size distribution and morphology need to be well defined. Compared with the usual methods, microwave synthesis has the advantages of short reaction time, small-size particles and narrow particle size distribution and high purity for preparing polycrystalline samples. Microwave energy is delivered directly to the material by molecular interactions under an electric field.

Therefore, it is possible to rapidly and uniformly heat thick materials. Cyclic microwave-assisted metathetic (MAM) synthesis of materials is a simple and cost-effective method that provides high yield with easy scale up and is emerging as a viable alternative approach for the synthesis of high-quality novel inorganic materials in short time periods^{4,20}. However, the microwave-assisted metathetic synthesis of the Fe₃O₄ incorporated BaMoO₄:Er³⁺/Yb³⁺ composites and their optical properties have not been reported. Therefore, the precise nature of the Fe₃O₄ incorporated BaMoO₄:Er³⁺/Yb³⁺ composites is required for a wide range of applications.

In this study, Fe₃O₄ incorporated Er³⁺ doped BaMoO₄ (BaMoO₄:Er³⁺) and Fe₃O₄ incorporated Er³⁺/Yb³⁺ co-doped BaMoO₄ (BaMoO₄:Er³⁺/Yb³⁺) composites were synthesized by the cyclic microwave-assisted metathetic route, followed by heat-treatment. The synthesized Fe₃O₄ incorporated BaMoO₄:Er³⁺ and Fe₃O₄ incorporated BaMoO₄:Er³⁺/Yb³⁺ composites were characterized by X-ray diffraction, scanning electron microscopy and energy-dispersive X-ray spectroscopy. Optical properties were examined by using photoluminescence emission data and Raman spectroscopy.

EXPERIMENTAL

Appropriate stoichiometric amounts of BaCl₂·2H₂O, ErCl₃·6H₂O, YbCl₃·6H₂O, Na₂MoO₄·2H₂O, 5 nm sized Fe₃O₄ nanoparticles and ethylene glycol of analytic reagent grade were used to prepare the Fe₃O₄ incorporated BaMoO₄:Er³⁺, Fe₃O₄ incorporated BaMoO₄:Er³⁺/Yb³⁺ and BaMoO₄:Er³⁺/Yb³⁺

compounds. For the preparation of Fe_3O_4 incorporated $\text{BaMoO}_4\cdot\text{Er}_3$, 0.95 mol % $\text{BaCl}_2\cdot 2\text{H}_2\text{O}$ with 0.05 mol % $\text{ErCl}_3\cdot 6\text{H}_2\text{O}$ and 1 mol % $\text{Na}_2\text{MoO}_4\cdot 2\text{H}_2\text{O}$ with 0.5 mol % Fe_3O_4 were dissolved in 30 mL ethylene glycol, respectively. To prepare Fe_3O_4 incorporated $\text{BaMoO}_4\cdot\text{Er}^{3+}/\text{Yb}^{3+}$, 0.9 mol % $\text{BaCl}_2\cdot 2\text{H}_2\text{O}$ with 0.05 mol % $\text{ErCl}_3\cdot 6\text{H}_2\text{O}$ and 0.05 mol % $\text{YbCl}_3\cdot 6\text{H}_2\text{O}$ and 1 mol % $\text{Na}_2\text{MoO}_4\cdot 2\text{H}_2\text{O}$ with 0.5 mol % Fe_3O_4 were dissolved in 30 mL ethylene glycol, respectively. In case of the preparation of $\text{BaMoO}_4\cdot\text{Er}^{3+}/\text{Yb}^{3+}$, 0.9 mol % $\text{BaCl}_2\cdot 2\text{H}_2\text{O}$ with 0.05 mol % $\text{ErCl}_3\cdot 6\text{H}_2\text{O}$ and 0.05 mol % $\text{YbCl}_3\cdot 6\text{H}_2\text{O}$ and 1 mol % $\text{Na}_2\text{MoO}_4\cdot 2\text{H}_2\text{O}$ were dissolved in 30 mL ethylene glycol, respectively.

The solutions were mixed and adjusted to pH 9.5 using NaOH. The aqueous solutions were stirred at room temperature. The mixtures were transferred into 120 mL Teflon vessels, respectively. Each Teflon vessel was placed into a microwave oven operating at a frequency of 2.45 GHz with a maximum output power of 1250 W for 23 min. The working cycle of the microwave-assisted metathetic reaction was controlled precisely between 30 s on and 30 s off for 8 min, followed by a further treatment of 30 s on and 60 s off for 15 min. The ethylene glycol was evaporated slowly at its boiling point. Ethylene glycol, a polar solvent at its boiling point of 197 °C, is a good candidate for the microwave process. When ethylene glycol is used as the solvent, reactions proceed at the boiling point temperature. The microwave radiation is supplied to ethylene glycol and the components dissolving in the ethylene glycol couple with each other under the radiation. When a large amount of microwave radiation is supplied to the ethylene glycol, the charged particles vibrate interdependently within the electric field. The resulting samples were treated with ultrasonic radiation and washed many times with hot distilled water. The white precipitates were collected and dried at 100 °C in a drying oven. The final products were heat-treated at 600 °C for 3 h.

The phase of the composites after the cyclic microwave-assisted metathetic reaction and heat-treatment was identified using XRD (D/MAX 2200, Rigaku, Japan). The microstructures and surface morphologies of the Fe_3O_4 incorporated $\text{BaMoO}_4\cdot\text{Er}^{3+}$ and Fe_3O_4 incorporated $\text{BaMoO}_4\cdot\text{Er}^{3+}/\text{Yb}^{3+}$ composites were observed by using SEM/EDS (JSM-5600, JEOL, Japan). Their photoluminescence spectra were recorded using a spectrophotometer (Perkin Elmer LS55, UK) at room temperature. Raman spectroscopy measurements were performed using a LabRam HR (Jobin-Yvon, France). The 514.5 nm line of an Ar-ion laser was used as the excitation source and the power on the samples was kept at 0.5 mW.

RESULTS AND DISCUSSION

Fig. 1 shows the XRD pattern of the synthesized Fe_3O_4 incorporated $\text{BaMoO}_4\cdot\text{Er}^{3+}/\text{Yb}^{3+}$ composites. The diffraction peaks marked with * are indexed to Fe_3O_4 . All of the XRD peaks could be assigned to the tetragonal-phase BaMoO_4 with a scheelite-type structure and Fe_3O_4 , which were in good agreement with the crystallographic data of BaMoO_4 (JCPDS 29-01930) and Fe_3O_4 (JCPDS 19-0629). It means that the Fe_3O_4 incorporated $\text{BaMoO}_4\cdot\text{Er}^{3+}/\text{Yb}^{3+}$ composites can be prepared using the cyclic microwave-assisted metathetic route. Post heat-

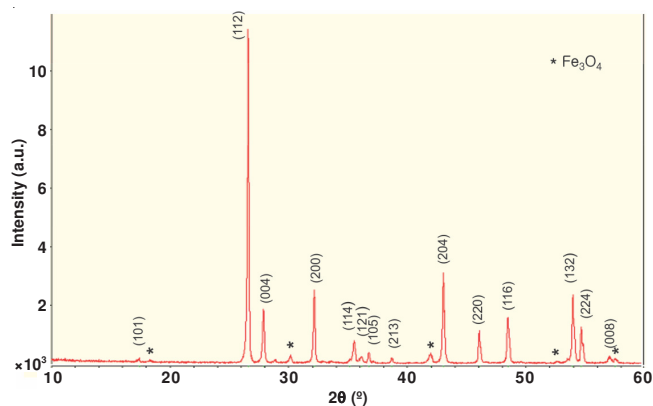


Fig. 1. XRD pattern of the synthesized Fe_3O_4 incorporated $\text{BaMoO}_4\cdot\text{Er}^{3+}/\text{Yb}^{3+}$ composites

treatment plays an important role in a well-defined crystallized morphology. To achieve a well-defined crystalline morphology, the Fe_3O_4 incorporated $\text{BaMoO}_4\cdot\text{Er}^{3+}$ and Fe_3O_4 incorporated $\text{BaMoO}_4\cdot\text{Er}^{3+}/\text{Yb}^{3+}$ composites need to be heat treated at 600 °C for 3 h. It suggests that the cyclic microwave-assisted metathetic route is suitable for growing Fe_3O_4 incorporated $\text{BaMoO}_4\cdot\text{Er}^{3+}$ and Fe_3O_4 incorporated $\text{BaMoO}_4\cdot\text{Er}^{3+}/\text{Yb}^{3+}$ composites and for developing the strongest intensity peaks at the (112), (204) and (312) planes, which are the major peaks of BaMoO_4 ^{4,6}.

Fig. 2 shows a SEM image of the synthesized Fe_3O_4 incorporated $\text{BaMoO}_4\cdot\text{Er}^{3+}/\text{Yb}^{3+}$ composites. The as-synthesized sample is a well-defined and homogeneous morphology with sizes of 1–2 μm for the $\text{BaMoO}_4\cdot\text{Er}^{3+}/\text{Yb}^{3+}$ particles and 0.1–0.5 μm for the Fe_3O_4 particles, respectively. The Fe_3O_4 particles were self-preferentially crystallized and immobilized on the surface of $\text{BaMoO}_4\cdot\text{Er}^{3+}/\text{Yb}^{3+}$ particles. Fig. 3 shows (a) a EDS pattern, (b) quantitative compositions, (c) quantitative results and (d) a SEM image of the synthesized Fe_3O_4 incorporated $\text{BaMoO}_4\cdot\text{Er}^{3+}/\text{Yb}^{3+}$ composites. The EDS pattern shows that the Fe_3O_4 incorporated $\text{BaMoO}_4\cdot\text{Er}^{3+}/\text{Yb}^{3+}$ composites are composed of Fe, Ba, Mo, O, Er and Yb in Fig. 3(a) and identified to the quantitative compositions in Fig. 3(b). The EDS pattern and quantitative compositions in Fig. 3 (a, b) could be assigned to the Fe_3O_4 incorporated $\text{BaMoO}_4\cdot\text{Er}^{3+}/\text{Yb}^{3+}$ composites. It means that the Fe_3O_4 nanoparticles incorporated $\text{BaMoO}_4\cdot\text{Er}^{3+}/\text{Yb}^{3+}$ composites can be successfully synthesized using this cyclic microwave-assisted metathetic. Microwave-assisted metathetic reactions, such as $\text{BaCl}_2 + \text{Na}_2\text{MoO}_4 \rightarrow \text{BaMoO}_4 + 2\text{NaCl}$, involve the exchange of atomic/ionic species, in which the driving force is the exothermic reaction accompanying the formation of NaCl ^{4,20}. Microwave-assisted metathetic reactions occur so rapidly that the exothermic reaction is essentially used to heat up the solid products. The cyclic microwave-assisted metathetic reactions provide a convenient route for the synthesis of Fe_3O_4 incorporated $\text{BaMoO}_4\cdot\text{Er}^{3+}$ and Fe_3O_4 incorporated $\text{BaMoO}_4\cdot\text{Er}^{3+}/\text{Yb}^{3+}$ composites. The cyclic microwave-assisted metathetic route²⁰ provides the exothermic energy to synthesize the bulk of the material uniformly, so that fine particles with controlled morphology can be fabricated in an environmentally friendly manner without the generation of solvent waste. Fe_3O_4 incorporated $\text{BaMoO}_4\cdot\text{Er}^{3+}$ and Fe_3O_4 incorporated $\text{BaMoO}_4\cdot\text{Er}^{3+}/\text{Yb}^{3+}$

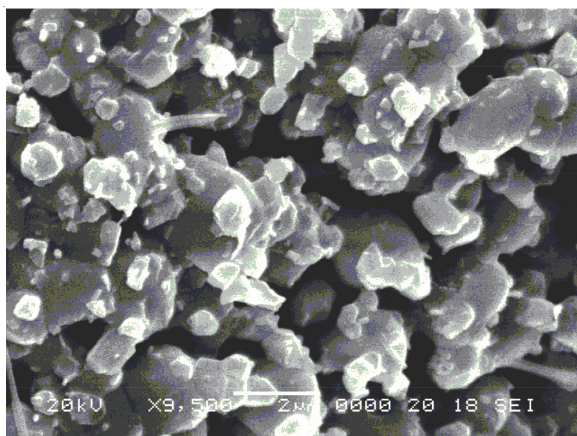


Fig. 2. SEM image of the synthesized Fe₃O₄ incorporated BaMoO₄:Er³⁺/Yb³⁺ composites

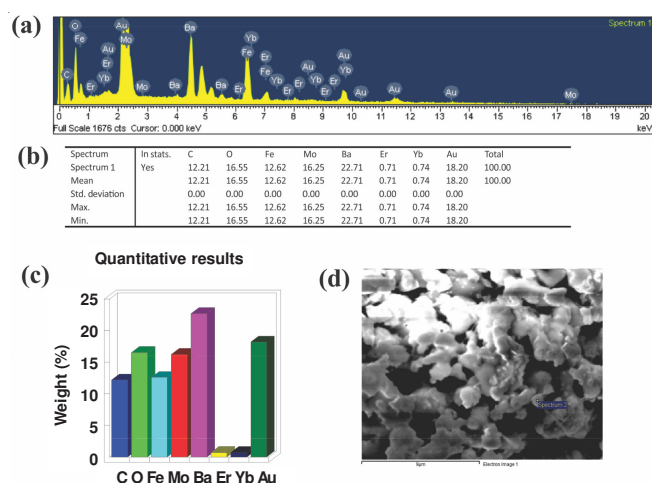


Fig. 3. (a) EDS pattern, (b) quantitative compositions, (c) quantitative results and (d) SEM image of the synthesized Fe₃O₄ incorporated BaMoO₄:Er³⁺/Yb³⁺ composites

composites were heated rapidly and uniformly by the cyclic microwave-assisted metathetic route. Therefore, this method is a simple and cost-effective method that can provide high yields with easy scale up, thus emerging as a viable alternative in the rapid synthesis of the Fe₃O₄ incorporated BaMoO₄:Er³⁺ and Fe₃O₄ incorporated BaMoO₄:Er³⁺/Yb³⁺ composites.

Fig. 4 shows the photoluminescence emission spectra of the synthesized (a) Fe₃O₄ incorporated BaMoO₄:Er³⁺ and (b) Fe₃O₄ incorporated BaMoO₄:Er³⁺/Yb³⁺ composites excited at 250 nm at room temperature. The emission spectrum of metal molybdates is due mainly to charge-transfer transitions within the [MoO₄]²⁻ complex^{21,22}. With excitation at 250 nm, the Fe₃O₄ incorporated BaMoO₄:Er³⁺ and Fe₃O₄ incorporated BaMoO₄:Er³⁺/Yb³⁺ composites exhibit a photoluminescence emission in the blue wavelength range of 370-420 nm. The photoluminescence intensity of the (b) Fe₃O₄ incorporated BaMoO₄:Er³⁺/Yb³⁺ is stronger than that of the (a) Fe₃O₄ incorporated BaMoO₄:Er³⁺. The doping amounts of Er³⁺/Yb³⁺ have an effect on the photoluminescence intensity. It suggests that the doping amounts play an important role in improving the luminescent efficiency. The photoluminescence intensity of energy-conversion materials depends strongly on not only the particle shape and distribution but also the doping amounts. Generally, for similar morphological samples, homogenized

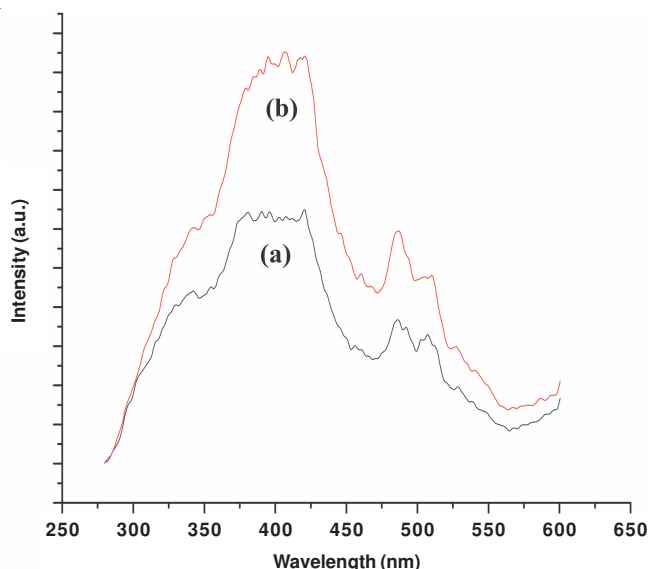


Fig. 4. Photoluminescence emission spectra of the synthesized (a) Fe₃O₄ incorporated BaMoO₄:Er³⁺ and (b) Fe₃O₄ incorporated BaMoO₄:Er³⁺/Yb³⁺ composites excited at 250 nm at room temperature

particles are favourable to the luminescent characteristics, because of the lesser contamination or fewer dead layers on the surface of the energy-conversion materials. The four narrow shoulders in the emission spectra at ca. 470, 490, 510 and 530 nm are believed to be due to a defect structure²³. Such peaks, namely the "spread-eagle" shape of the blue emission, can be explained by the influence of the Jahn-Teller effect^{24,25} on the degenerated excited state of the [MoO₄]²⁻ tetrahedron. Generally, the presence of Gaussian components indicates that the electronic levels corresponding to the relaxed excited state of an emission centre belong to a degenerate excited state influenced by some perturbation, e.g., a local low symmetry crystal field²³. The Jahn-Teller splitting effect essentially determines the emission shape of the MMoO₄ (M = Ca, Ba) particles. The additional emission bands can be explained by the existence of a Frenkel defect structure (oxygen ion shifted to the interposition with the simultaneous creation of vacancies) in the surface layers of the BaMoO₄ particles²⁶.

Fig. 5 shows Raman spectra of the synthesized (a) BaMoO₄:Er³⁺/Yb³⁺ (BMO:ErYb) particles and (b) Fe₃O₄ incorporated BaMoO₄:Er³⁺/Yb³⁺ (F-BMO:ErYb) composites excited by the 514.5 nm line of an Ar-ion laser at 0.5 mW on the samples. The Raman spectra show that the peak positions are same, while the intensities of (a) BaMoO₄:Er³⁺/Yb³⁺ (BMO:ErYb) is slightly higher than that of (b) Fe₃O₄ incorporated BaMoO₄:Er³⁺/Yb³⁺ (F-BMO:ErYb). The internal modes for the (a) BaMoO₄:Er³⁺/Yb³⁺ (BMO:ErYb) particles and (b) Fe₃O₄ incorporated BaMoO₄:Er³⁺/Yb³⁺ (F-BMO:ErYb) composites were detected as ν₁(A_g), ν₃(B_g), ν₃(E_g), ν₄(E_g), ν₄(B_g) and ν₂(B_g) vibrations at 891, 838, 791, 359, 346 and 325 cm⁻¹, respectively. A free rotation mode was detected at 187 cm⁻¹ and the external modes were localized at 140 and 107 cm⁻¹. The internal vibration mode frequencies are dependent on the lattice parameters and the degree of the partially covalent bond between the cation and molecular ionic group [MoO₄]²⁻. The Raman spectra of the synthesized BaMoO₄:Er³⁺/Yb³⁺ (BMO:ErYb) particles and Fe₃O₄ incorporated BaMoO₄:Er³⁺/

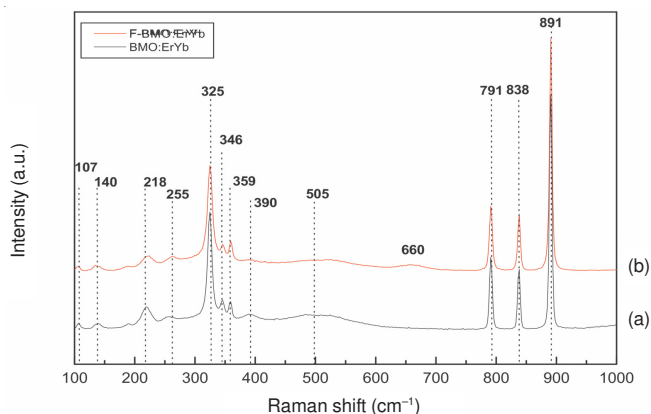


Fig. 5. Raman spectra of the synthesized (a) $\text{BaMoO}_4:\text{Er}^{3+}$ (BMO:ErYb) particles and (b) Fe_3O_4 incorporated $\text{BaMoO}_4:\text{Er}^{3+}/\text{Yb}^{3+}$ (F-BMO:ErYb) composites excited by the 514.5 nm line of an Ar-ion laser at 0.5 mW on the samples

Yb^{3+} (F-BMO:ErYb) composites indicate additional peaks at both higher frequencies (505 and 390 cm^{-1}) and lower frequencies (255 and 218 cm^{-1}), which are attributed to the doping ion of $\text{Er}^{3+}/\text{Yb}^{3+}$. It is noted that the Fe_3O_4 particles have no influence on the Raman spectra, while the doping ion of $\text{Er}^{3+}/\text{Yb}^{3+}$ can influence the Raman spectra. The Raman spectra proved that the doping ion of $\text{Er}^{3+}/\text{Yb}^{3+}$ can influence the structure of the host materials.

Conclusion

Fe_3O_4 incorporated $\text{BaMoO}_4:\text{Er}^{3+}/\text{Yb}^{3+}$ composites were successfully synthesized by a cyclic microwave-assisted metathetic route. The microstructure exhibited a well-defined and homogeneous morphology with sizes of 1-2 μm for the $\text{BaMoO}_4:\text{Er}^{3+}/\text{Yb}^{3+}$ particles and 0.1-0.5 μm for the Fe_3O_4 particles, respectively. The Fe_3O_4 particles were self-preferentially crystallized and immobilized on the surface of $\text{BaMoO}_4:\text{Er}^{3+}/\text{Yb}^{3+}$ particles. With excitation at 250 nm, the Fe_3O_4 incorporated $\text{BaMoO}_4:\text{Er}^{3+}$ and Fe_3O_4 incorporated $\text{BaMoO}_4:\text{Er}^{3+}/\text{Yb}^{3+}$ composites exhibited a photoluminescence emission in the blue wavelength range of 370-420 nm. The photoluminescence intensity of the Fe_3O_4 incorporated $\text{BaMoO}_4:\text{Er}^{3+}/\text{Yb}^{3+}$ was stronger than that of the Fe_3O_4 incorporated $\text{BaMoO}_4:\text{Er}^{3+}$. The doping amounts of $\text{Er}^{3+}/\text{Yb}^{3+}$ had an effect on the photoluminescence intensity. The Raman spectra of the synthesized $\text{BaMoO}_4:\text{Er}^{3+}/\text{Yb}^{3+}$ (BMO:ErYb) particles and Fe_3O_4 incorporated $\text{BaMoO}_4:\text{Er}^{3+}/\text{Yb}^{3+}$ (F-BMO:ErYb) composites indicated additional peaks at both higher frequencies (505 and 390 cm^{-1}) and lower frequencies (255 and 218 cm^{-1}), which were attributed to the doping ion of $\text{Er}^{3+}/\text{Yb}^{3+}$. The Raman spectra proved that the doping ion of $\text{Er}^{3+}/\text{Yb}^{3+}$ can influence the structure of the host materials.

ACKNOWLEDGEMENTS

This study was supported by Basic Science Research Program through the National Research Foundation of Korea (NRF) funded by the Ministry of Education, Science and Technology (2012-0007858).

REFERENCES

1. D. Liu, L. Tong, J. Shi and H. Yang, *J. Alloys Comp.*, **512**, 361 (2012).
2. L. Liu, L. Xiao and H.Y. Zhu, *Chem. Phys. Lett.*, **539-540**, 112 (2012).
3. Q. Wang, X. yang, L. Yu and H. Yang, *J. Alloys Comp.*, **509**, 9098 (2011).
4. C.S. Lim, *J. Lum.*, **132**, 1774 (2012).
5. J.H. Ryu, J.W. Yoon, C.S. Lim and K.B. Shim, *Mater. Res. Bull.*, **40**, 1468 (2005).
6. J.H. Ryu, K.M. Kim, S.W. Min, G.S. Park, J.W. Yun, K.B. Shim and C.S. Lim, *Appl. Phys. A*, **92**, 407 (2008).
7. X. Lin, X. Qiao and X. Fan, *Solid State Sci.*, **13**, 579 (2011).
8. L.Y. Zhou, J.S. Wei, F.Z. Gong, J.L. Huang and L.H. Yi, *J. Solid State Chem.*, **181**, 1337 (2008).
9. J. Liu, H. Lian and C. Shi, *Opt. Mater.*, **29**, 1591 (2007).
10. X. Li, Z. Yang, L. Guan, J. Guo, Y. Wang and Q. Guo, *J. Alloys Comp.*, **478**, 684 (2009).
11. D. Gao, Y. Li, Y. Wei, J. Bi, Y. Li and M. Liu, *Mater. Chem. Phys.*, **126**, 391 (2011).
12. Y. Yang, X. Li, W. Feng, W. Yang, W. Li and C. Tao, *J. Alloys Comp.*, **509**, 845 (2011).
13. F.B. Cao, L.S. Li, Y.W. Tian, Y.J. Chen and X.R. Wu, *Thin Solid Films*, **519**, 7971 (2011).
14. Y. Jin, J. Zhang, Z. Hao, X. Zhang and X.J. Wang, *J. Alloys Comp.*, **509**, L348 (2011).
15. F. Yu, J. Zuo, Z. Zhao, C. Jiang and Q. Yang, *Mater. Res. Bull.*, **46**, 1327 (2011).
16. F. Lei and B. Yan, *J. Solid State Chem.*, **181**, 855 (2008).
17. Z.J. Zhang, H.H. Chen, X.X. Yang and J.T. Zhao, *Mater. Sci. Eng. B*, **145**, 34 (2007).
18. N. Niu, P. Yang, W. Wang, F. He, S. Gai, D. Wang and J. Lin, *Mater. Res. Bull.*, **46**, 333 (2011).
19. J. Zhang, X. Wang, X. Zhang, X. Zhao, X. Liu and L. Peng, *Inorg. Chem. Commun.*, **14**, 1723 (2011).
20. C.S. Lim, *Mater. Chem. Phys.*, **131**, 714 (2012).
21. D.A. Spassky, S.N. Ivanov, V.N. Kolobanov, V.V. Mikhailin, V.N. Zemskov, B.I. Zadneprovski and L.I. Potkin, *Radiat. Meas.*, **38**, 607 (2004).
22. G.Y. Hong, B.S. Jeon, Y.K. Yoo and J.S. Yoo, *J. Electrochem. Soc.*, **148**, H161 (2001).
23. K. Polak, M. Nikl, K. Nitsch, M. Kobayashi, M. Ishii, Y. Usuki and O. Jarolimek, *J. Lumin.*, **72-74**, 781 (1997).
24. Y. Toyozawa and M. Inoue, *J. Phys. Soc. (Japan)*, **21**, 1663 (1966).
25. E.G. Reut, *Izv. Akad. Nauk SSSR Ser. Fiz.*, **43**, 1186 (1979).
26. V.B. Mikhailik, H. Kraus, D. Wahl and M.S. Mykhaylyk, *Phys. Status Solid B*, **242**, R17 (2005).